

Comparative Analysis of Fully Reusable Launch Vehicles: Fuel Choices and Landing Architectures

Jascha Wilken^{*†}, Moritz Herberhold^{*}, Dr. Martin Sippel^{*}

^{*} Institute of Space Systems, DLR

Robert-Hooke -Str.7 28359 Bremen, Germany

Jascha.wilken@dlr.de

[†] Corresponding Author

Abstract

Fully reusable two-stage-to-orbit (TSTO) launch vehicles, such as SpaceX's Starship, are poised to reshape the future of space access. Yet, systematic design studies of this architecture remain scarce, particularly in the European context. This paper addresses that gap through a parametric assessment of key design variables: propellant type, engine cycle, and stage propellant ratio. A unified modelling framework combines mass estimation, ascent trajectory optimization, and booster recovery analysis to explore performance across multiple configurations. The goal is to build an understanding of Starship-class systems and assess their applicability to future European heavy-lift development.

1 Introduction

Over the past decade, global launch providers have begun to embrace partial reusability, with a strong focus on recovering first stages. In contrast, SpaceX is advancing towards the first fully reusable orbital launch system with Starship—a vehicle architecture that could fundamentally reshape the space launch market, much as Falcon 9 did before it. Although Starship still faces considerable technical hurdles, its long-term impact on launch economics and system design is already becoming apparent.

Starship's design is shaped by SpaceX's long-term ambition of enabling human missions to Mars. However, this interplanetary goal imposes requirements that may not align with the needs of launch systems optimized for Earth-orbit missions, especially those serving near-term commercial or institutional markets. For any competitor considering a similar architecture—particularly within Europe—it is essential to understand which design choices are intrinsic to the fully reusable concept and which are specific to Mars-oriented use cases.

While reusable booster stages have been the subject of detailed trade studies [1], examining factors such as propellant choice, engine cycle, and recovery strategy, there is a noticeable lack of equivalent studies for fully reusable two-stage-to-orbit (TSTO) systems. This paper explores this gap by evaluating key design parameters and performance sensitivities of Starship-like vehicles through a systematic parametric approach.

The breadth of this study precludes a detailed analysis of each configuration. A comparison and discussion of specific heavy lift options for Europe including fully reusable launch vehicles can be found in [5].

1.1 Horizontal landing

As a possible variation on the Starship architecture, herein the possibility of landing horizontally (HL) is investigated in addition to the vertical landing (VL) approach chosen by SpaceX. The idea is to keep as much commonality between the concepts as possible, including the fuselage and the propulsion system. The HL configuration shall be equipped with the hardware necessary to safely land, which includes for example larger wings, landing gear and a sizable fin. For SpaceX this approach is not of interest due to the final goal of landing on Mars, but this constraint doesn't apply to systems focused on other missions. The target of this analysis is not the derivation of a converged design, but instead to check if this type of architecture even is of interest and warrants further investigation.

2 Methods

The following sections outline the modelling framework developed to assess fully reusable two-stage launch vehicles. Since the primary objective is to compare payload performance across a range of staging configurations, the workflow begins with a defined propulsion system and specified propellant loading for each stage. From these inputs, key vehicle

characteristics—including geometry, mass, aerodynamics, and trajectory, are derived in a consistent manner to enable meaningful comparisons across architectures.

2.1 Geometry

The size of each stage is determined by the volume required to contain its assigned propellant mass, assuming constant length-to-diameter ratios: 7 for the first stage and 5 for the second stage. This approach preserves geometric similarity to the original Starship design but leads to differing diameters between the stages, particularly in configurations with extreme propellant ratios. While an alternative method could enforce a uniform overall length-to-diameter ratio, this would distort individual stage proportions and result in unrealistic geometries when deviating significantly from the Starship baseline.

Aerodynamic surfaces are scaled proportionally with stage length to maintain comparable aerodynamic characteristics across propellant loadings.

2.2 Aerodynamic properties

While the study considers the full mission profile, only the ascent phase is modelled through numerical trajectory integration. For this reason, the aerodynamic database from [4], developed for the full Starship configuration, is applied during ascent. Other flight phases, such as the booster return, are handled through analytical approximations that do not require a detailed aerodynamic model. Although HL (horizontal-landing) configurations introduce larger aerodynamic surfaces, their impact on ascent drag and thus performance is expected to be minimal and will be addressed in future higher-fidelity analyses.

For this initial investigation, the final wing shape of the MDO performed in [6] was adopted and scaled with the vehicle length. An initial check with the DLR tool *cac* showed sufficient lift generation to land at under 100 m/s, similar to the Space Shuttle. For the hypersonic performance, the trimability of the configuration is of importance but was not considered at this stage. In subsequent analysis with regard to the center of gravity position and the pitch trimability of the vehicle, it is likely that the wing shape will have to be modified. However, the overall size of the wing is likely dictated by the landing requirement, discussed in [6], and thus this is a good starting point for the subsequent design iterations.

Sketches of the aerodynamic configurations of the upper stages for VL and HL are shown in Figure 1.

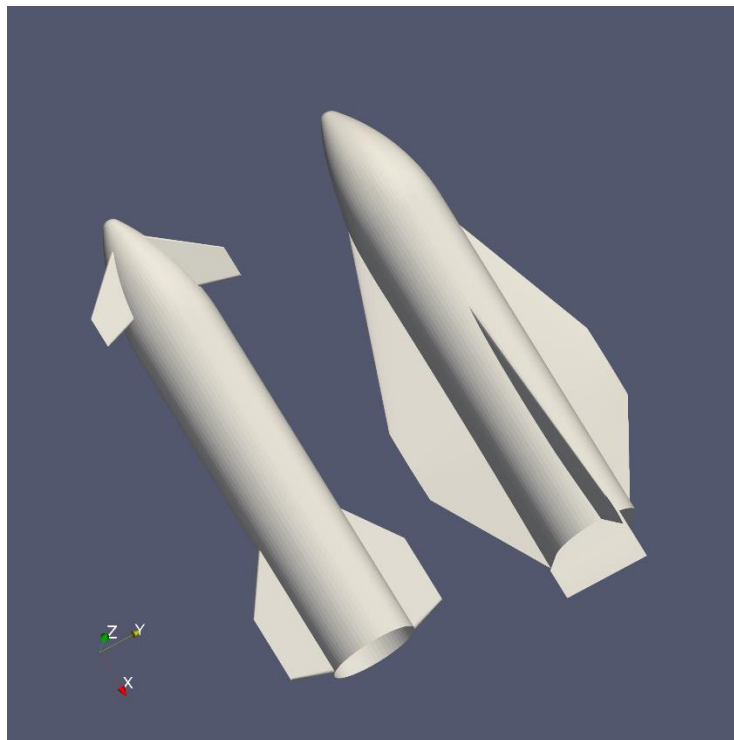


Figure 1: Sketches of geometries used for mass model of VL (left) and HL (right) reusable upper stages

2.3 Propulsion

A total of five propulsion systems are evaluated in this study. Their performance and mass characteristics are summarized in Table 1. These include one system based on publicly available and internally derived data for SpaceX's Raptor 3 [4], and four configurations drawn from the ENTRAIN engine reference set [2], representing potential European developments.

- **Raptor-3:** Based on SpaceX's methane-fueled staged-combustion engine. While DLR internal recalculations closely reproduce SpaceX's published performance figures, the estimated engine mass differs significantly. Stochastic mass-scaling models cannot replicate the unusually low mass values claimed by SpaceX[3]. For consistency and comparability, this study uses the DLR-derived estimates for both performance and mass.
- **ENTRAIN engines:** Sourced from the ENTRAIN study's reference datasets, these configurations reflect realistic targets for future European engine developments. The staged-combustion variants assume moderate main combustion chamber pressures (MCCP) (160 bar), compared to the 350 bar targeted by SpaceX's Raptor 3. Further technical details and assumptions for these engines are documented in [2].
 - ENTRAIN C SC: Methane-fueled staged-combustion engine
 - ENTRAIN C GG: Methane-fueled gas-generator engine
 - ENTRAIN H SC: Hydrogen-fueled staged-combustion engine
 - ENTRAIN H GG: Hydrogen-fueled gas-generator engine.

Table 1: Propulsion datasets of the five propulsion options investigated within this study

		Raptor 3 - like	ENTRAIN C SC	ENTRAIN C GG	ENTRAIN H SC	ENTRAIN H GG
Fuel		LCH4	LCH4	LCH4	LH2	LH2
Total engine mixture ratio [-]		3.6	3.25	2.5	6	6
MCCP [bar]		350	160	120	160	120
Sea level engine	Sea level Isp [s]	329	314	289	394	367
	Vac Isp [s]	348	343	320	428	405
	Expansion Ratio [-]	32	23	20	23	20
	Tvac/w [-]	92.3	76.6	105	74.6	98.6
Vacuum engine	Vac Isp [s]	366	366	348	459	440
	Expansion Ratio [-]	100	120	120	120	120
	Tvac/W [-]	85.6	70.6	85.2	70.2	82.4

For all configurations presented in the following sections, engine thrust is sized to ensure a thrust-to-weight ratio (T/W) of 1.45 at liftoff and 1.0 at second-stage ignition. This approach may yield non-integer engine ratios between the two stages. In practical implementations—particularly those intending to share engine hardware across stages—some deviation from these thrust levels may be necessary to accommodate discrete engine counts.

For vertically landing upper stages, it is assumed that half of the engines are sea-level variants with shortened nozzles, enabling propulsive landing capability. For the HL configuration it is assumed that all engines of the upper stage are of the vacuum variant with larger expansion ratios. This leads to an increase in the effective specific impulse of 2-4%, compared to the VL upper stages.

Another aspect not considered at this stage, is the engine accommodation. The assumed thrust levels are fairly high, and it is possible that fitting all necessary engines within the first stage diameter will be challenging, as is already the case in the actual Starship. This will likely be most critical for the methane fueled configurations, as the hydrogen fueled configurations benefit (in this aspect) from the lower density of the fuel and likely have sufficient space for whatever thrust level is required.

2.4 Mass model

Assuming a given propellant loading, the dry mass of each configuration was estimated with the DLR tool *stsm*, which uses parametric functions based on historical data to estimate the mass of individual components. The model makeup is very similar to the Starship reverse engineering results shown and discussed in [4].

The propellants are always assumed to be densified but still entirely liquid. The aerodynamic surfaces are scaled with stage length, for the VL version these are the forward and rearward flaps, for the HL version these are the wings, flaps, the fin and the body flap.

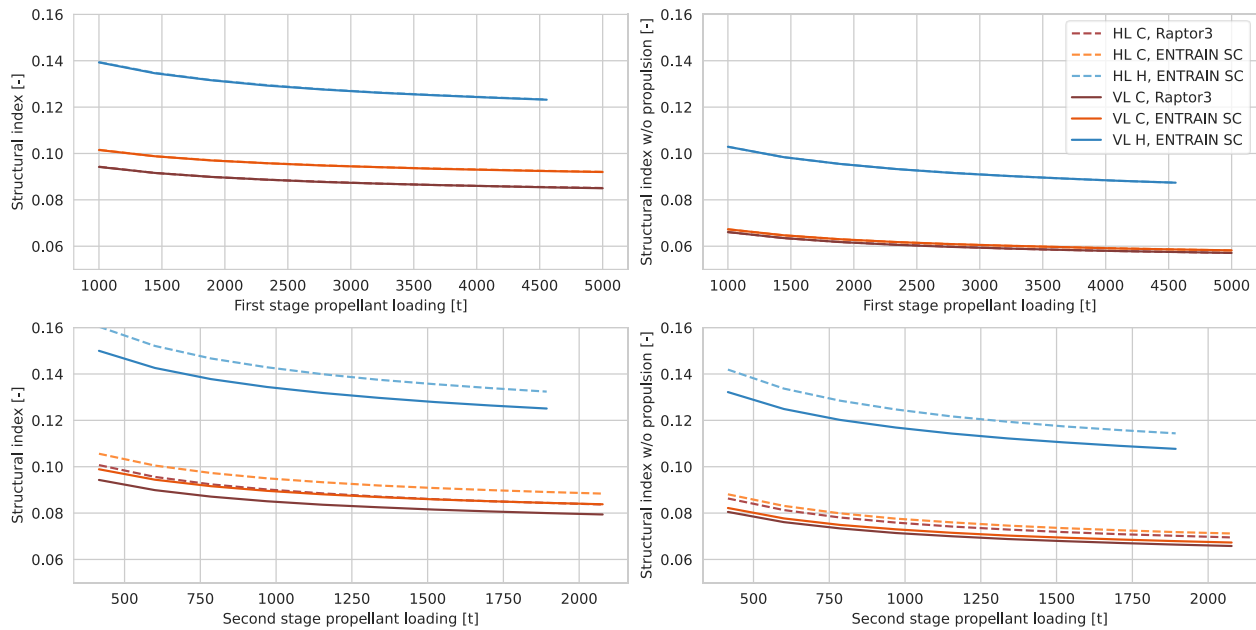


Figure 2: Structural index over propellant loading for first and second stages, with and without propulsion system

The structural indexes, assuming a propellant ratio identical to the Starship V2 (3650t/1500t) with and without the main rocket engines are shown in Figure 2. The actual values used in the parametrical studies shown in the results section differ slightly, as the upper stage has an impact on the dry mass of the first stage (for example through the thrust requirements at lift-off).

For the first stage, barely any difference between the VL and HL versions can be seen, which is expected as the first stages are identical in both cases. Only minor changes are caused by the higher dry mass of the second stage, which in turn causes slightly increased lift-off thrust and engine mass (since the T/W is set to 1.45).

Between the Raptor 3 and ENTRAIN C SC variant there is a small difference in structural index, caused by the lower T/W of the ENTRAIN engines. A smaller difference remains even in the structural index without main propulsion, since the dry mass of the engines affects other components.

For the upper stages, a difference can be seen between the VL and HL configurations. The impact of the larger wing size of the HL configuration is not as large as might be expected, since the airfoil thickness also significantly increases. The VL configuration has fairly thin wings, the airfoil thickness at the wing root is almost 5x as large for the HL configuration, which has a positive effect on the mass estimation with the underlying analytic formulas. Thus, the wings of the HL are heavier, but the mass doesn't linearly scale with planform area. For the case shown in the sketch in Figure 1, where the fuselage length corresponds to the Starship V3, the mass of the aerodynamic surfaces of the HL configuration is $\sim 2.7x$ the mass of the aerodynamics surfaces of the VL configuration (excluding the TPS in both cases, but including flaps, actuators and fins). However, in neither case are the aerodynamic surfaces major mass drivers, these can be found in the payload bay, the propellant tanks and the propulsion system.

2.5 Payload performance

For this initial parametric survey, only the ascent trajectory is numerically integrated and optimized. The propellant required for the first stage's return-to-launch-site (RTLS) maneuver is estimated analytically. It is assumed that the boost-back burn cancels both the vertical and horizontal velocity of the stage and provides the acceleration necessary

to initiate the return arc toward the launch site. This approximation has been validated against publicly available Starship performance data, as described in [4].

This model reflects the current Super Heavy return profile, where a single boost-back burn accomplishes both velocity cancellation and return trajectory shaping. This differs from the Falcon 9 approach, in which only the horizontal velocity is reversed and the stage follows a high ballistic arc, decelerated later by a reentry burn. In contrast, Super Heavy does not currently employ a dedicated reentry burn. Instead, it relies on aerodynamic braking and the final landing burn. As SpaceX continues to refine its recovery profile, including potential changes in stage separation and descent dynamics, the associated propellant demands may also evolve.

The analytical return model allows the required descent propellant to be accounted for during ascent optimization. Stage separation is triggered precisely when the remaining onboard propellant is sufficient for the full return sequence. This way, the optimizer implicitly incorporates return fuel constraints when shaping the pitch maneuver and angle-of-attack history.

The launch is assumed to take place in Boca Chica, the target orbit is a 250x300km LEO with 26° inclination. Trajectory integration is carried out using DLR's Tosca tool [7], with the py-cma package [8] providing external optimization via the CMA-ES algorithm.

3 Results

A first comparison of the performance of various propulsion options for a fixed propellant loading is shown in section 3.1 and a more comprehensive parametric variation of the propellant loading of both stages is shown in section 3.2.

3.1 Initial exploration

As an initial sizing exercise, a fixed propellant load, 3650 t in the first stage and 1500 t in the second stage, was applied to four representative propulsion systems across two propellant types. The resulting low Earth orbit (LEO) payload capacities are summarized in Table 2.

Table 2: Payload performance for various propulsion system with identical propellant loading (3650 t in first and 1500 t in second stage)

Propulsion	Fuel	Payload - VL configuration	Payload - HL configuration
Raptor 3	Methane	115 t	139 t
ENTRAIN C SC	Methane	96 t	122 t
ENTRAIN C GG	Methane	55 t	82 t
ENTRAIN H SC	Hydrogen	215 t	245 t
ENTRAIN H GG	Hydrogen	175 t	207 t

The most striking result is the significant spread in performance among the methane-fueled configurations. Even between two staged-combustion engines—Raptor-3 and ENTRAIN C SC—the difference in payload exceeds 20%, largely due to the much higher main combustion chamber pressure of the Raptor. Switching from staged combustion to a gas-generator cycle results in an even more severe drop: the ENTRAIN C GG configuration delivers less than half the payload of the Raptor-based version, underscoring the critical impact of engine cycle efficiency and chamber pressure when using hydrocarbon propellants.

While the hydrogen-fueled variants achieve substantially higher payloads for the same propellant mass, this comes at the cost of significantly larger vehicle dimensions. The required stage diameters reach 12.7 m for the booster and 12.4 m for the upper stage, driven by hydrogen's low density. This results in a total tank volume increase of roughly 2.4× compared to the methane-based cases, with corresponding impacts on structural mass, aerodynamic drag, and ground infrastructure complexity.

Alternative comparison methods, such as holding total propellant volume constant or matching payload performance, can offer additional insight into the trade-offs between fuels. These perspectives are explored in subsequent parametric studies of propellant loading and staging ratios.

3.2 Staging exploration

While the fixed-propellant evaluation provides a useful initial comparison of engine cycle and fuel choice impacts, applying the same reference loading across all configurations can introduce distortions. Different propellants, along

with their associated tankage, performance, and structural penalties, may result in distinct optimal stage propellant ratios. Moreover, to fully understand and compare the staging behavior of each architecture, a broader exploration of the trade space is required.

To address this, a parametric study was conducted in which the propellant loading of both stages was systematically varied. The same modelling and optimization methods described earlier were used to evaluate each configuration across this extended design space.

This variation focused on the closed cycles engines, excluding the gas generator propulsion systems. The initial exploration already allows a good assessment of their performance relative to the staged combustion engine systems.

The payload performances and the payload fraction for each investigated propellant loading is shown in the following figures. While the range in propellant loading varies significantly, the overall pattern in the results is similar (and is expected): With rising propellant loading the payload performance also increases. It can be seen that a certain ratio of propellant loading in each stage leads to increased payload fractions, but also that a larger propellant loading leads to higher payload ratios, as the structural indexes of the stages are reduced.

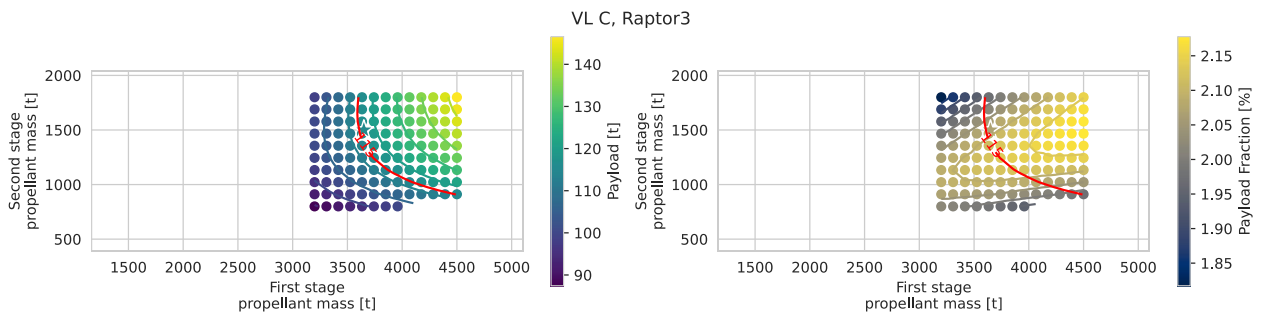


Figure 3: Parametric study of first and second stage propellant masses for the VL Raptor 3 configuration. Line of 115 t payload performance (into LEO) is indicated in red.

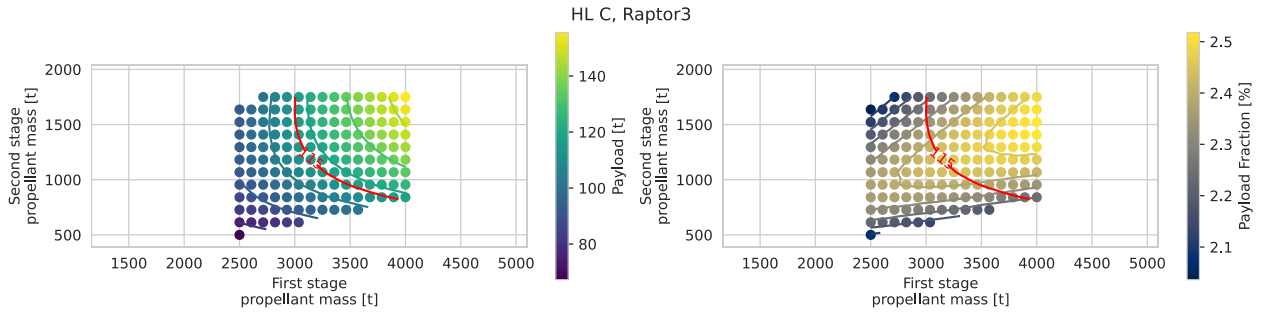


Figure 4: Parametric study of first and second stage propellant masses for the HL Raptor 3 configuration. Line of 115 t payload performance (into LEO) is indicated in red.

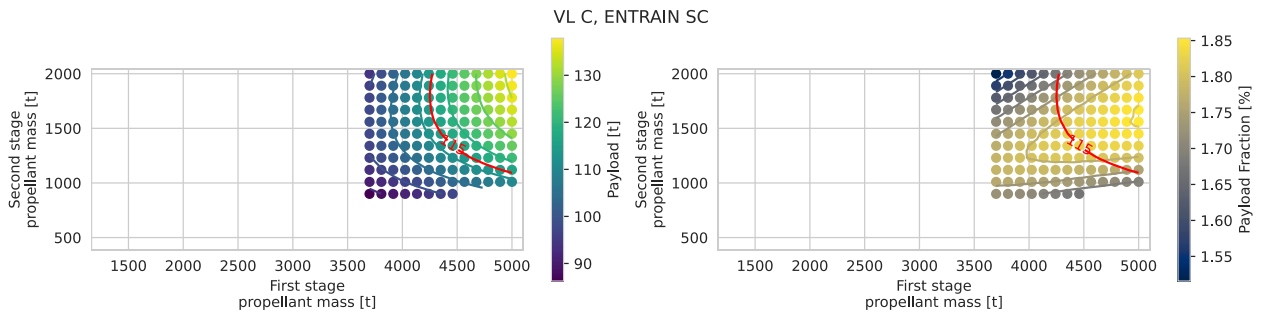


Figure 5: Parametric study of first and second stage propellant masses for the VL C ENTRAIN SC configuration. Line of 115 t payload performance (into LEO) is indicated in red.

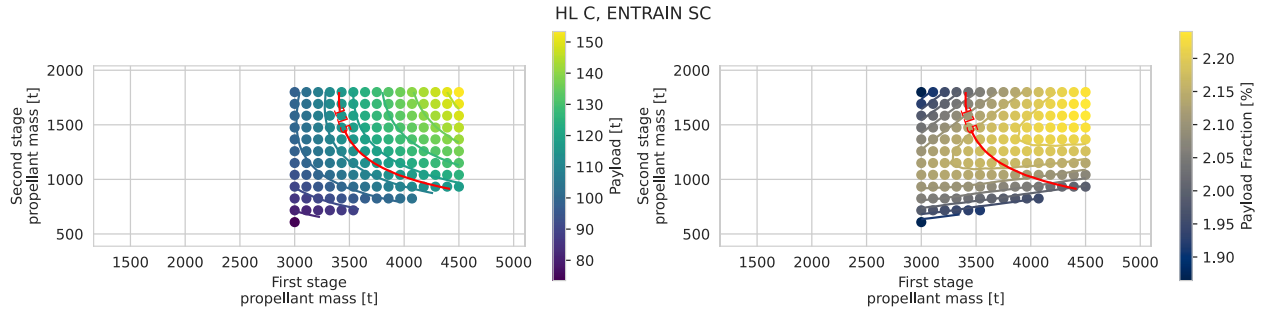


Figure 6: Parametric study of first and second stage propellant masses for the HL CC ENTRAIN SC configuration. Line of 115 t payload performance (into LEO) is indicated in red.

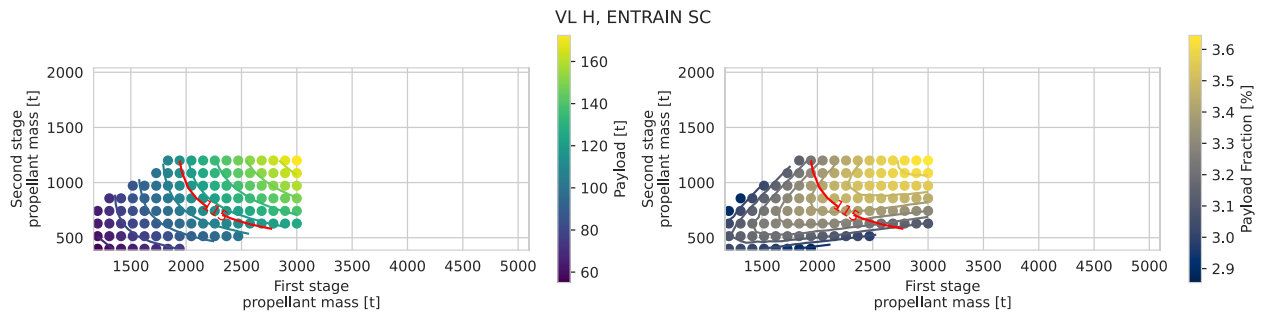


Figure 7: Parametric study of first and second stage propellant masses for the VL HH ENTRAIN SC configuration. Line of 115 t payload performance (into LEO) is indicated in red.

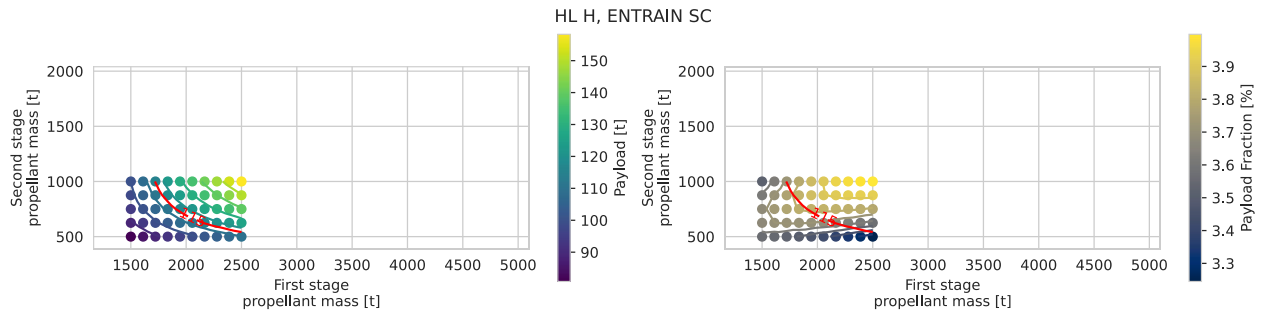


Figure 8: Parametric study of first and second stage propellant masses for the HL HH ENTRAIN SC configuration. Line of 115 t payload performance (into LEO) is indicated in red.

3.2.1 Comparison for fixed payload performance

Using the results shown above, the properties of launch vehicles for a given payload performance can be interpolated from the surrounding data points. This was done for a required performance of 115 t, in order to compare the resulting properties of various propellant ratios. Where applicable, the values resulting from the Starship V2 propellant loading (3650t in the first and 1500t in the second stage) are shown for reference.

In Figure 9 the resulting total mass is shown over the ratio of propellant in first and second stage. Overall, the expected trends are observed: significantly less propellant is required when using hydrogen as fuel. For methane-fueled vehicles, employing higher-performance Raptor 3-like engines leads to notably lighter designs, with the most pronounced differences seen in the VL configurations.

In general, HL configurations are lighter than their VL counterparts, and this disparity increases with higher specific impulse. The effect is especially evident in the ENTRAIN C SC configurations.

Optimal staging in terms of minimizing total mass occurs at lower propellant ratios (i.e. larger upper stages) for hydrogen-fueled cases compared to methane-fueled ones. Similarly, in HL configurations, the minimum total mass tends to shift toward designs with larger upper stages, likely due to their higher specific impulse, as the VL variants incorporate sea-level engines in the upper stage for landing, which reduces overall efficiency.

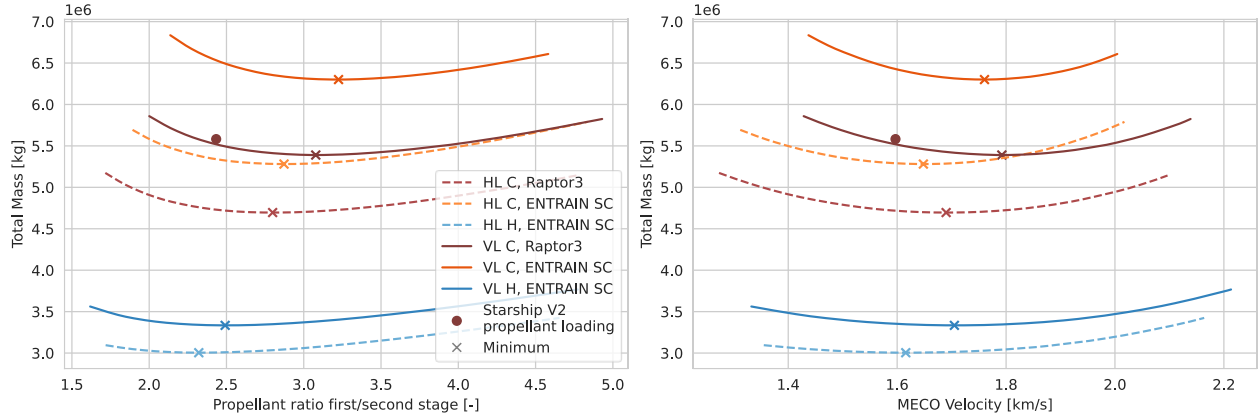


Figure 9: Total mass over propellant ratio (left) and stage separation velocity (right), for different propulsion systems delivering a 115 t payload to LEO

Also, in Figure 9, the total mass is shown over the resulting stage separation velocity. Remarkably, across all propulsion architectures examined, the separation velocity corresponding to the minimal total mass consistently falls within a narrow range of 1.6 to 1.8 km/s.

An interesting trend emerges when comparing optimal staging for configurations using ENTRAIN C SC versus Raptor 3-like engines: with the higher-performance Raptor 3-like engines, a smaller portion of the total propellant is allocated to the first stage, yet these configurations still achieve higher stage separation velocities. This highlights the influence of the Raptor 3-like engines' higher combustion chamber pressure on improving performance, particularly at low altitudes.

Figure 10 shows the propellant volume over the propellant ratio of first to second stage and over the stage separation velocity.

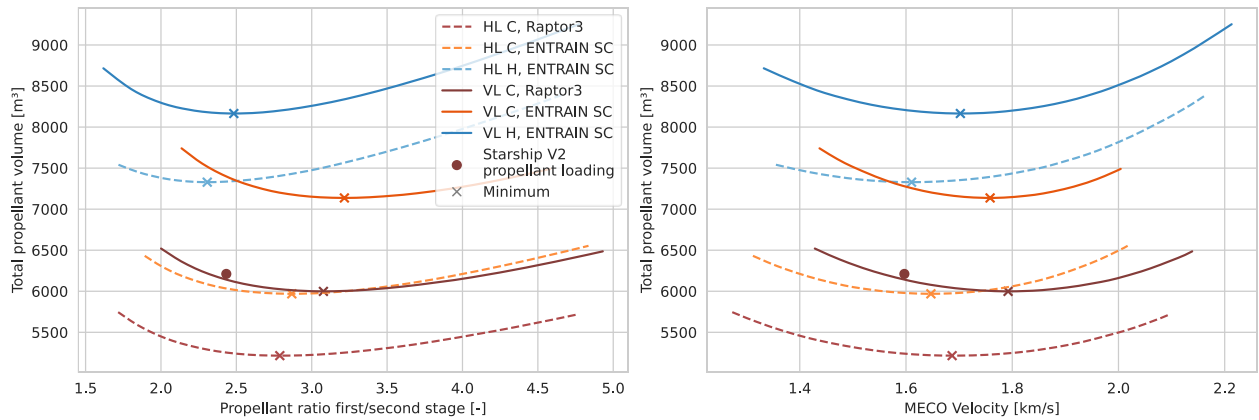


Figure 10: Total propellant volume over propellant ratio (left) and stage separation velocity (right), for different propulsion systems delivering a 115 t payload to LEO

It can be seen that the hydrogen fueled configurations need more propellant volume for the same mission. This is in contrast to the results previously published in the ENTRAIN study [1]. There, launch vehicles with reusable first stages were compared for different fuels and it was consistently found that the hydrogen fueled vehicles were not only lighter but also smaller than the methane fueled equivalents. Two reasons are identified for this differing result:

- Lower total Δv : In the ENTRAIN study the target was a Geo-Transfer Orbit (GTO), which necessitates a total Δv budget that is higher than the budget needed for the LEO targeted herein, even when including the propellant needed for the RTLS. As velocity requirements increase, hydrogen becomes increasingly advantageous due to its higher specific impulse compared to methane.
- Large geometry-dependent additional masses: In the ENTRAIN study, upper stages were expendable, resulting in efficient designs with relatively low dry masses and a fairing that was jettisoned as soon as heat flux conditions permitted. In contrast, the upper stage architecture examined in this study includes extensive recovery hardware and a large, fixed payload bay. Because these components are scaled based on vehicle

geometry rather than propellant mass, their weight is more closely tied to propellant volume. This leads to comparatively higher structural indices, particularly for hydrogen-fueled configurations.

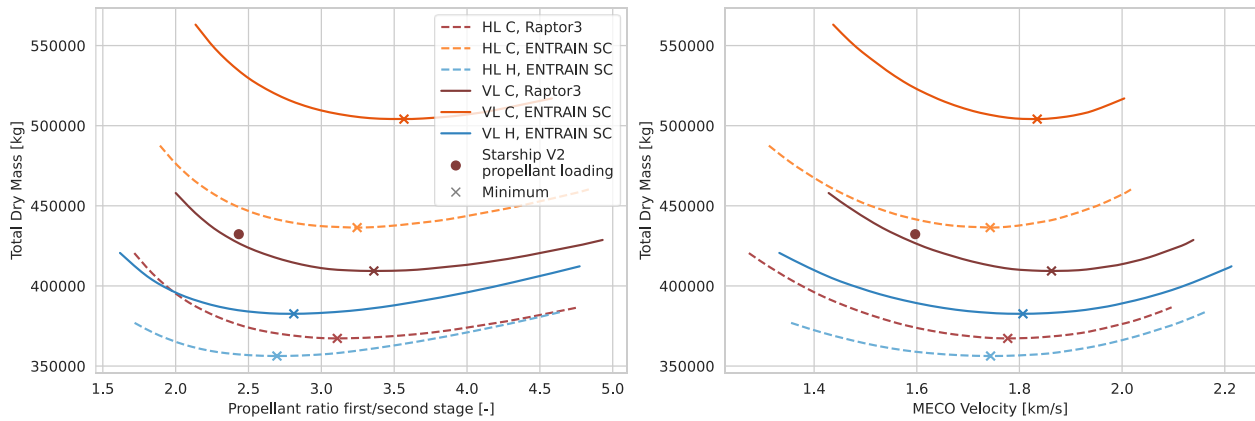


Figure 11: Total dry mass over propellant ratio (left) and stage separation velocity (right), for different propulsion systems delivering a 115 t payload to LEO

Beyond total mass, total dry mass is also a key metric, serving as a first-order indicator of development and production costs. Figure 11 presents total dry mass as a function of the propellant ratio and stage separation velocity. The points of minimal dry mass tend to occur at higher separation velocities compared to those of minimal total mass. This is primarily because the first stage typically exhibits lower structural indices than the second stage.

While hydrogen-fueled stages yield the lowest dry masses overall, the difference compared to methane-fueled configurations is less pronounced than in the case of total mass. This is particularly evident in methane configurations utilizing propulsion parameters based on the high-performance Raptor 3 engine.

Consistent with total mass trends, HL configurations generally exhibit lower dry masses than their VL counterparts. Even though their structural indexes are higher, the lower total propellant mass more than compensates this. This advantage becomes more significant as the specific impulse of the propulsion system decreases.

The exact economic optimum will likely depend on the relative costs of recovery and refurbishment for the two reusable stages. Given that the upper stage experiences significantly higher thermal loads, its refurbishment is expected to be more expensive per unit mass. As a result, the cost-optimal separation velocity may exceed the point of minimal dry mass.

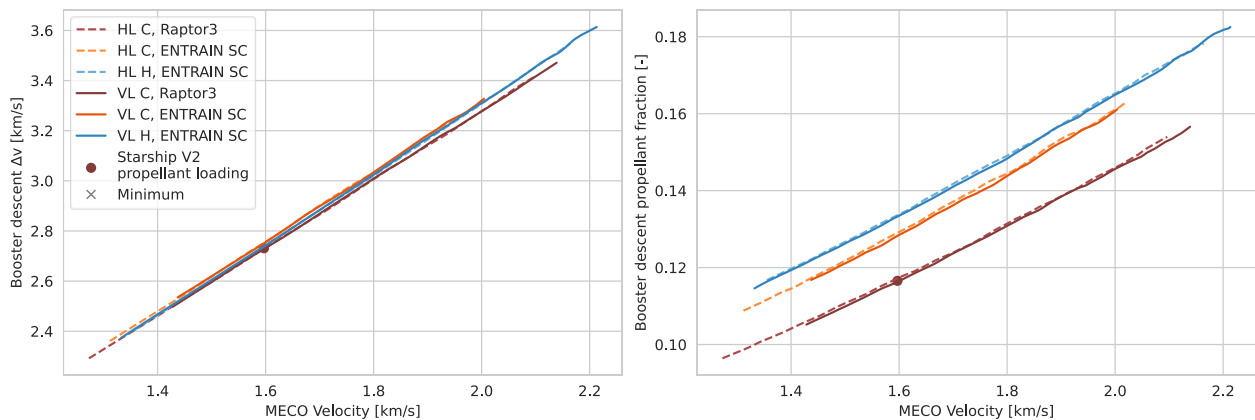


Figure 12: Descent Δv (left) and descent propellant fraction (right) over stage separation velocity, for different propulsion systems delivering a 115 t payload to LEO

An interesting observation can be made when comparing the fraction of first stage propellant used for the return and landing, shown in Figure 12 alongside the actual Δv of the maneuver: Even though the hydrogen fueled configurations have a higher specific impulse, they actually need to use a larger fraction of their first stage propellant for the RTLS maneuver, due to the higher structural indexes.

The nearly identical descent Δv values result from simplifications in the analytical approximation. In practice, hydrogen-fueled stages are likely to require slightly less Δv for descent, owing to their lower ballistic coefficients during reentry. This allows them to make more effective use of aerodynamic deceleration.

4 Discussion

In this study, the architecture of the fully reusable Starship of SpaceX was explored and the effect of multiple design changes analyzed. As propulsion systems, both the values given for the high-performance engine Raptor 3 with 350 bar MCCP and values derived for possible future European developments are assessed.

From the results it is clear that simply copying the architecture without achieving the same engine performance comes with substantial performance losses. Over 20% of the payload performance is lost, even using a closed cycle engine with a lower MCCP. Relying on gas generator engines instead leads to over 50% payload performance loss.

With regard to the propellants, hydrogen fueled variants were found to deliver the same payload with lower total and lower dry mass. However, for the dry mass, the methane fueled variant with the Raptor 3 engine achieves similar total dry mass than the 160 bar MCCP European hydrogen fueled engines.

The possibility of landing the upper stage horizontally appears promising. While this requires a larger and thus heavier wing, a heavier thermal protection system, and a landing gear, this is more than balanced by the saving in landing fuel and the ability to use entirely vacuum optimized engines in the second stages. The largest possible benefit is for the propulsion systems with lowest specific impulse. However, the aerodynamic shape of the horizontally landing version is still under investigation and the hypersonic trimability has to be confirmed (see also the outlook in chapter 5). For SpaceX this approach is not of interest since the atmosphere of Mars is too thin to realistically land horizontally. However, for other future adaptations of the architecture focused on Earth-to-orbit, or Earth-to-Earth transport this type of fully reusable launch vehicle should be considered, especially if the available propulsion technology cannot match the impressive performance of the Raptor 3.

While not the focus of this work, the recovery mode of the SuperHeavy booster is likely with little alternative. Concepts like In-Air-Capturing, while promising for smaller stages [1], do not easily scale to this size. Vertically landing the stage on a ship also is likely challenging at this scale and might incur substantial operational costs. Nonetheless, this recovery method for the first stage imposes low separation velocities. While the separation velocity is sufficient for the LEO orbits targeted in this study, it will be very challenging to achieve substantial payload performance to higher orbits. Thus, this space transportation architecture essentially requires some type of in-orbit transportation network, be it dedicated orbital transfer vehicles or the refueling strategy pursued by SpaceX.

4.1 Comparison to SpaceX Starship staging

The optimal staging identified in the results shown in section 3.2, differs from the staging chosen by SpaceX for its future Starship V2 iteration. Possible reasons for this are manifold: A shift in the structural index from one stage to another could lead to this, or constraints on the size of the first stage.

Another possible constraint is Starship's actual target mission: The transfer to Mars. While the exact number depends on the launch window and the envisaged travel time, it seems likely that this mission imposes a minimum Δv requirement on the Starship stage, even if the first stage would be able to deliver a higher fraction of the Δv .

While the staging does differ from the actual values, in general the analysis does confirm the low staging velocities chosen by SpaceX. These are lower than found in the operational ELV vehicles but similar to the separation velocities found in the current RTLS missions of the Falcon 9.

5 Outlook

As noted in chapter 2.2, the aerodynamic configuration of the horizontally landing configurations is not converged. While the mass model accounts for the wing size, no trimming analysis has been performed. This will likely require the change of the wing shape or position, but is not expected to have a large impact on the mass budget.

A particular challenge is the potential inclusion of the capability of returning mass from orbit to Earth. Since the payload bay is located at the front of the second stage, returning any substantial mass from orbit would likely result in a significant forward shift of the center of gravity. The VL configuration, with its two pairs of flaps, may offer greater flexibility in accommodating this shift.

However, if the current HL wing configuration proves insufficient to manage such changes in mass distribution, modifications to the aerodynamic design could be explored. Possible options include the addition of canards or relocating a main propellant tank toward the front of the vehicle to enable a centrally positioned payload bay. This would help mitigate the impact of returned payload mass on the overall center of gravity.

LLM-Assisted Text Revision

During the preparation of this work, the author used ChatGPT 4o in order to revise the text. After using this tool/service, the author reviewed and edited the content as needed and takes full responsibility for the content of the publication.

6 References

- [1] Dietlein, I., Bussler, L., Stappert, S. et al. Overview of system study on recovery methods for reusable first stages of future European launchers. CEAS Space J 17, 71–88 (2025). <https://doi.org/10.1007/s12567-024-00557-9>
- [2] Sippel, M., Wilken, J. Selection of propulsion characteristics for systematic assessment of future European RLV-options. CEAS Space J 17, 89–111 (2025). <https://doi.org/10.1007/s12567-024-00564-w>
- [3] SpaceX, "Performance Stats of Raptor," 3 08 2024. [Online]. Available: <https://x.com/spacex/status/1819795288116330594>. [Accessed 25 06 2025].
- [4] Herberhold, M., Bussler, L., Sippel, M. et al. Comparison of SpaceX's Starship with winged heavy-lift launcher options for Europe. CEAS Space J (2025). <https://doi.org/10.1007/s12567-025-00625-8>
- [5] Sippel, M., Herberhold, M., Bergmann, K., Dietlein, I., Bussler, L.: Future Reusable Launcher Options for Europe: The Heavy Class Segment. EUCASS 2025, 2025
- [6] Tommaso Acta Paper Mauriello, Tommaso und Wilken, Jascha und Callsen, Steffen und Bussler, Leonid und Sippel, M.: Multidisciplinary Design Analysis and Optimization Of The Aerodynamic Shape Of The Spaceliner Passenger Stage. Acta Astronautica. Elsevier. doi: 10.1016/j.actaastro.2024.07.054, ISSN 0094-5765.
- [7] H. Kayal, "Aufbau eines vereinfachten Simulationsmodells für den Bahnaufstieg in der Großkreisebene," 1993. Available: <https://elib.dlr.de/23152/>.
- [8] Nikolaus Hansen, Youhei Akimoto, and Petr Baudis. CMA-ES/pycma on Github. Zenodo, DOI:10.5281/zenodo.2559634, 2019.